Early Onset of Age-Related Cataracts in Cystine/Glutamate Antiporter Knockout Mice

Renita Maria Martis,[1,2] Bo Li,[1,2] Paul James Donaldson,[1,2] and Julie Ching-Hsia Lim[1,2]

[1]Department of Physiology, School of Medical Sciences, University of Auckland, Auckland, New Zealand
[2]New Zealand National Eye Centre, University of Auckland, Auckland, New Zealand

Correspondence: Julie C. Lim, Department of Physiology, School of Medical and Health Sciences, University of Auckland, 85 Park Road, Grafton, Auckland, 1023, New Zealand; j.lim@auckland.ac.nz.

Received: March 29, 2021
Accepted: May 24, 2021
Published: June 22, 2021

Citation: Martis RM, Li B, Donaldson PJ, Lim JC-H. Early onset of age-related cataracts in cystine/glutamate antiporter knockout mice. *Invest Ophthalmol Vis Sci.* 2021;62(7):23. https://doi.org/10.1167/iovs.62.7.23

Purpose. The purpose of this study was to determine the importance of the xCT is a subunit. The cystine/glutamate antiporter is actually system xc-xCT subunit of the cystine/glutamate antiporter in maintaining redox balance by investigating the effects of the loss of xCT on lens transparency and cystine/cysteine balance in the aqueous humour.

Methods. C57Bl/6 wild-type and xCT knockout mice at five age groups (6 weeks to 12 months) were used. Lens transparency was examined using a slit-lamp and morphological changes visualized by immunolabelling and confocal microscopy. Quantification of glutathione in lenses and cysteine and cystine levels in the aqueous was conducted by liquid chromatography tandem mass spectrometry (LC-MS/MS).

Results. Slit-lamp examinations revealed that 3-month-old wild-type mice and xCT knockout mice lenses exhibited an anterior localized cataract. The frequency of this cataract significantly increased in the knockout mice compared to the wild-type mice. Morphological studies revealed a localized swelling of the lens fiber cells at the anterior pole. Glutathione levels in whole lenses were similar between wild-type and knockout mice. However, glutathione levels were significantly decreased at 3 months in the knockout mice in the lens epithelium compared to the wild-type mice. Aqueous cysteine levels remained similar between wild-type and knockout mice at all age groups, whereas cystine levels were significantly increased in 3-, 9-, and 12-month-old knockout mice compared to wild-type mice.

Conclusions. Loss of xCT resulted in the depletion of glutathione in the epithelium and an oxidative shift in the cysteine/cystine ratio of the aqueous. Together, these oxidative changes may contribute to the accelerated development of an anterior cataract in knockout mice, which appears to be a normal feature of aging in wild-type mice.

Keywords: cataract, cystine/glutamate exchanger (xCT), glutathione, lens, oxidative stress

The cystine/glutamate antiporter (system xc-) is responsible for mediating the uptake of extracellular cystine in exchange for the export of intracellular glutamate.[1] It is a member of the heteromeric amino acid transporter family and comprised of two subunits; a functional light chain known as xCT, that is responsible for the transport of the amino acids, and a heavy chain subunit known as 4F2hc, which anchors the transporter to the plasma membrane.

xCT has been shown to be expressed in the brain,[2–9] plus the kidneys, liver, and lungs.[10,11] These studies have revealed xCT to play a number of important roles. These include (i) the uptake of cystine, which is subsequently reduced to cysteine for the use in the synthesis of the antioxidant glutathione, (ii) the regulation of the extracellular cystine/cysteine redox balance through driving uptake of cystine to maintain a cystine/cysteine redox cycle, and finally (iii) the modulation of extracellular glutamate levels either for neurotransmission and/or providing tonic stimulation for metabotropic glutamate receptors.[3]

xCT is also expressed in different tissues of the eye, such as the cornea (rat, mouse, and human), the ciliary body (rat and mouse), the lens (rat, mouse, canine, and human), and the retina (rat, mouse, and human).[12–22] In cultured human corneal epithelial cells, retinal pigment epithelial cells, and lens epithelial cells, pharmacological inhibition of xCT has been shown to result in reduced glutathione (GSH) depletion, pointing to a role for xCT in maintaining GSH levels in these cells.[14,16,17] Localization studies of xCT in the rat and human cornea also indicate a role for xCT in GSH synthesis,[21,23] while co-localization of xCT to the synaptic ribbon complex in the rat retina suggests a role for xCT in glutamate neurotransmission.[15] However, the actual in vivo role(s) of xCT in the different tissues of the eye are still unknown.

In previous work, we used the use of a global xCT knockout mouse[24] to confirm the expression of xCT in the mouse lens (see Supplementary Fig. S1). We revealed that in the lens, xCT expression is restricted to the epithelium and cortical fiber cells,[22] the regions of the lens capable of de novo protein synthesis, a location that was suggestive of a role for xCT in mediating GSH synthesis. In addition, similar to that reported by Sato and colleagues,[24] we showed that at 6 weeks of age while plasma cysteine levels were

similar between wild-type mice (WT) and xCT knockout (xCT KO) mice, cystine levels were significantly increased in the xCT KO mice relative to the WT mice, indicative of an oxidative shift in the extracellular environment.[22] Moreover, we also revealed that in the aqueous humour, cystine levels were significantly higher in the young xCT KO mouse compared to the WT mouse, mirroring the oxidative shift in the plasma induced by the loss of xCT in the xCT KO mouse.[22]

The purpose of this study is to elucidate the effects of loss of xCT on lens morphology and transparency, lens intracellular GSH levels, and aqueous cystine/cysteine levels with advancing age (from 6 weeks to 12 months of age). Our findings revealed that loss of xCT results in the accelerated development of an anterior localized cataract at 3 months of age, reduced levels of GSH in the lens epithelium at 3 months of age, and cystine/cysteine redox imbalance in the aqueous humour of mice for all age groups. This suggests that xCT plays an important role in preserving a reduced extracellular environment and maintaining GSH levels in the lens epithelium and that loss of xCT exposes the lens to a heightened oxidative environment resulting in the accelerated progression of a distinctive cataract phenotype.

Methods

Animals

All animals were treated in accordance with protocols approved by the University of Auckland Animal Ethics Committee (Ethics number R001893) and the ARVO Statement for the Use of Animals in Ophthalmic and Vision Research. The xCT KO mice used in this study were descendants of the strain previously described.[24] All xCT KO mice were healthy in appearance, fertile, and lived a normal lifespan.[24] Wild type (WT) C57BL/6J mice were used as controls. Mice used in this study were either male or female of 6 weeks, 3 months, 6 months, 9 months, or 12 months of age.

Genotyping

Genotyping was performed as described by Sato and colleagues[24] and verified by PCR of tail DNA in our laboratory, as previously stated.[22]

Slit Lamp Examination

Animals were anaesthetized intraperitoneally using a combination of ketamine (75 mg/kg) and medetomidine (1.0 mg/kg). Animals were then placed on a heating pad set to 37°C, which was orientated to 45 degreees, and the eye placed precisely 27 mm from the objective lens of the Micron IV slit lamp attachment (Phoenix Research Lab, Pleasanton, CA, USA) in order to ensure equal magnification of the eye between animals. Images of the lens were captured using retro-illumination and parallelepiped illumination. Optical coherence tomography (OCT) images of the lens were taken using the OCT attachment and fundus lens. Quantification of the cataract lesion area (mm^2) was performed using the retro-illuminated images in combination with ImageJ 1.46r (Wayne Rasband, National Institutes of Health, Bethesda, MD, USA).

Lens Collection and Tissue Preparation

For quantification of metabolites and oxidative stress markers, eyes were enucleated and placed in prewarmed 37°C PBS. Eyes were then dissected and the whole lens carefully removed and placed in a prechilled Eppendorf tube containing 50 mM EDTA (Sigma-Aldrich, Darmstadt, Germany). For lens fractions, the epithelium, cortex, and nucleus were dissected on a prechilled petri dish and transferred to a prechilled Eppendorf tube containing 50 mM EDTA. Aqueous humour was collected as previously described.[22] Whole lens and fractions were then homogenized, spun down at 16,000 rcf for 20 minutes at 4°C, supernatant collected, snap frozen, and stored at −80°C. WT and xCT KO mice samples (lens and aqueous humour) for each age group were collected together and stored at -80°C for no more than 1 week. Samples for each age group were then divided into two or more batches and analyzed on different days to ensure there was no processing or instrumentation errors. WT and xCT KO mice samples were always processed together from each group.

Metabolite Quantification of Cysteine/Cystine in the Aqueous Humour and GSH/GSSG in the Lens

Liquid chromatography tandem mass spectrometry (LC-MS/MS) was used to quantify cysteine and cystine and/or reduced GSH and oxidized GSH (GSSG) in WT and xCT KO mice samples collected from aqueous humour and lens homogenates at each of the different age groups. Aqueous humour cysteine/cystine levels were measured using established methods.[22] To measure total GSH (GSH + GSSG) and GSH in whole or fractionated lenses, isotopically labelled GSH (13C) derivatized with MBrB at a final concentration of 4.92 µM was used. The processed samples were then directed into the QSTAR XL Quadrupole-Time-of-Flight mass spectrometer with the following transitions: GSH-MBrB (498.17 → 225.07) and 13C GSH -MBrB (501.17 → 225.07). Reduced GSH and total GSH were quantified from their extracted ion chromatograms and comparison to the labeled standard, and GSSG concentrations quantified by subtraction of GSH from total cysteine or total GSH.

Quantification of Oxidative Stress Markers

4-HNE and Protein Carbonyls Quantification. To measure lipid peroxidation 4-hydroxynonenal (4-HNE), OxiSelect HNE Adduct Competitive ELISA kits were purchased from Cell Biolabs (San Diego, CA, USA). To quantify protein carbonyl levels, a commercially available ELISA-based assay kits was used (BioCell Corporation, Auckland, New Zealand). Whole lenses were first homogenized in 50 mM EDTA and spun at 16,000 rcf for 20 minutes at 4°C; supernatants were collected and stored at -80°C. Samples were first thawed out before being processed and analyzed as per the manufacturer's instructions.

Immunohistochemistry

Lenses were dissected and immediately fixed as previously reported.[25] For α-SMA labeling, a protocol employed by Nowak and colleagues,[26] was adapted, and optimized to fix the lenses without dissection from the eye. To do this, a small incision was first made at the corneal limbus and posterior pole of the enucleated eye, before placing the

Investigative Ophthalmology & Visual Science

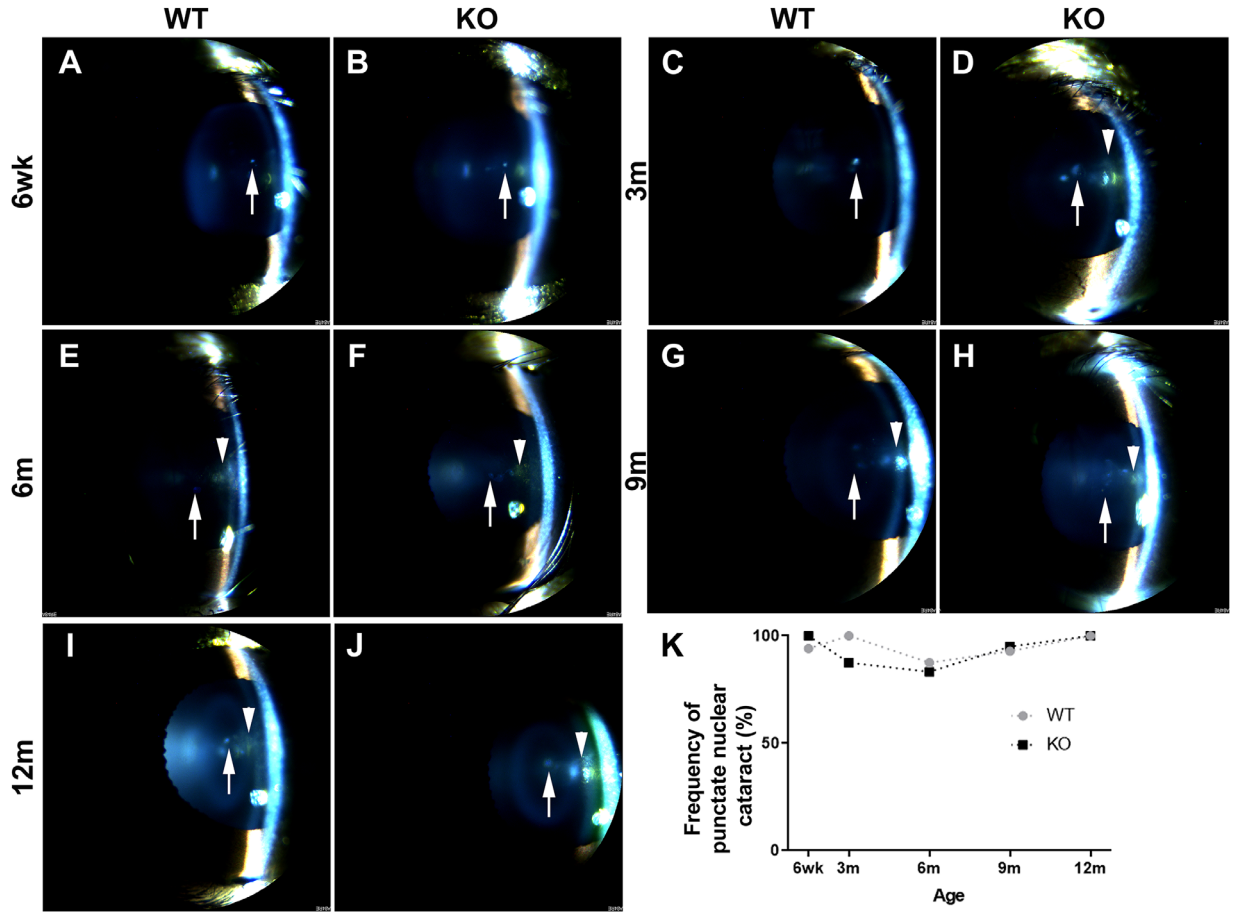

Figure 1. Parallelepiped examination of the lenses of wild-type and xCT knockout mice. Mice were anaesthetized, pupils dilated, and lenses examined in vivo with a slit lamp where the defects were assessed under parallelepiped illumination. Representative images of the lenses observed in wild-type (WT) and knockout (KO) mice at (**A, B**) 6 weeks, (**C, D**) 3 months, (**E, F**) 6 months, (**G, H**) 9 months, and (**I, J**) 12 months of age. *Arrows* highlight punctate nuclear cataracts in the nucleus. *Arrowheads* highlight the anterior cataract. (**K**) Images of lenses captured were used to quantify the frequency of the punctate nuclear lesions in WT (*grey*) and KO (*black*) mice; $n = 17$ WT and 18 KO mice at 6 weeks, 10 WT and 8 KO mice at 3 months, 8 WT and 6 KO mice at 6 months, 28 WT and 20 KO mice at 9 months, and 18 WT and 17 KO mice eyes at 12 months.

whole eye in 1% w/v PFA for 24 hours. Fixed lenses were dissected from the eye, cryoprotected, sectioned, and labeled as previously described.[25] For α-SMA labeling, sections were washed, and then incubated with α-SMA antibodies (1:200; Sigma-Aldrich, Darmstadt, Germany) overnight at 4°C. Sections were then labeled with Alexa Fluor 488 (1:200; Life Technologies, Carlsbad, CA, USA), washed, and then incubated in 4',6-diamidino-2-phenylindole (DAPI; 1:1000) and wheat germ agglutinin conjugated to an Alexa Fluor 594 (WGA; 1:100). Sections were then mounted with VECTASHIELD HardSet aqueous mounting medium (Vector Laboratories, Burlingame, CA, USA), and imaged using the Olympus FV1000 confocal laser scanning microscope (Olympus Corporation, Tokyo, Japan). Raw data were processed and merged if required using Adobe Photoshop CS6 version 13.0 (Adobe Systems Pty. Inc., San Francisco, CA, USA).

Statistical Analysis

All numerical values (Supplementary Table S1) and graphs are displayed as mean ± standard error of the mean (SEM) unless otherwise stated. To compare changes with age and genotype for all experiments, a 2-way ANOVA test was first conducted to determine statistical significance. Once significance was confirmed, a Tukey's post hoc analysis was conducted to ascertain significance between each group using GraphPad Prism version 8. The P values stated are from the Tukey's multiple comparison test. To compare the frequency of lenses affected with cataract, a χ^2 test was conducted. The P values of < 0.05 were considered statistically significant. The following is used to state significance $^*P < 0.05$, $^{**}P < 0.01$, $^{***}P < 0.001$, or $^{****}P < 0.0001$.

Results

In Vivo Ocular Examinations of WT and xCT KO Mice

In order to determine the effect loss of xCT on lens transparency, we performed in vivo slit lamp microscopy on cohorts of WT and xCT KO mice at 6 weeks, 3 months, 6 months, 9 months, and 12 months of age. Two regionally distinct cataracts were identified, a punctate nuclear cataract (Fig. 1; indicated by the arrows) and an anterior cataract (Fig. 1, Fig. 2; indicated by the arrowheads) that

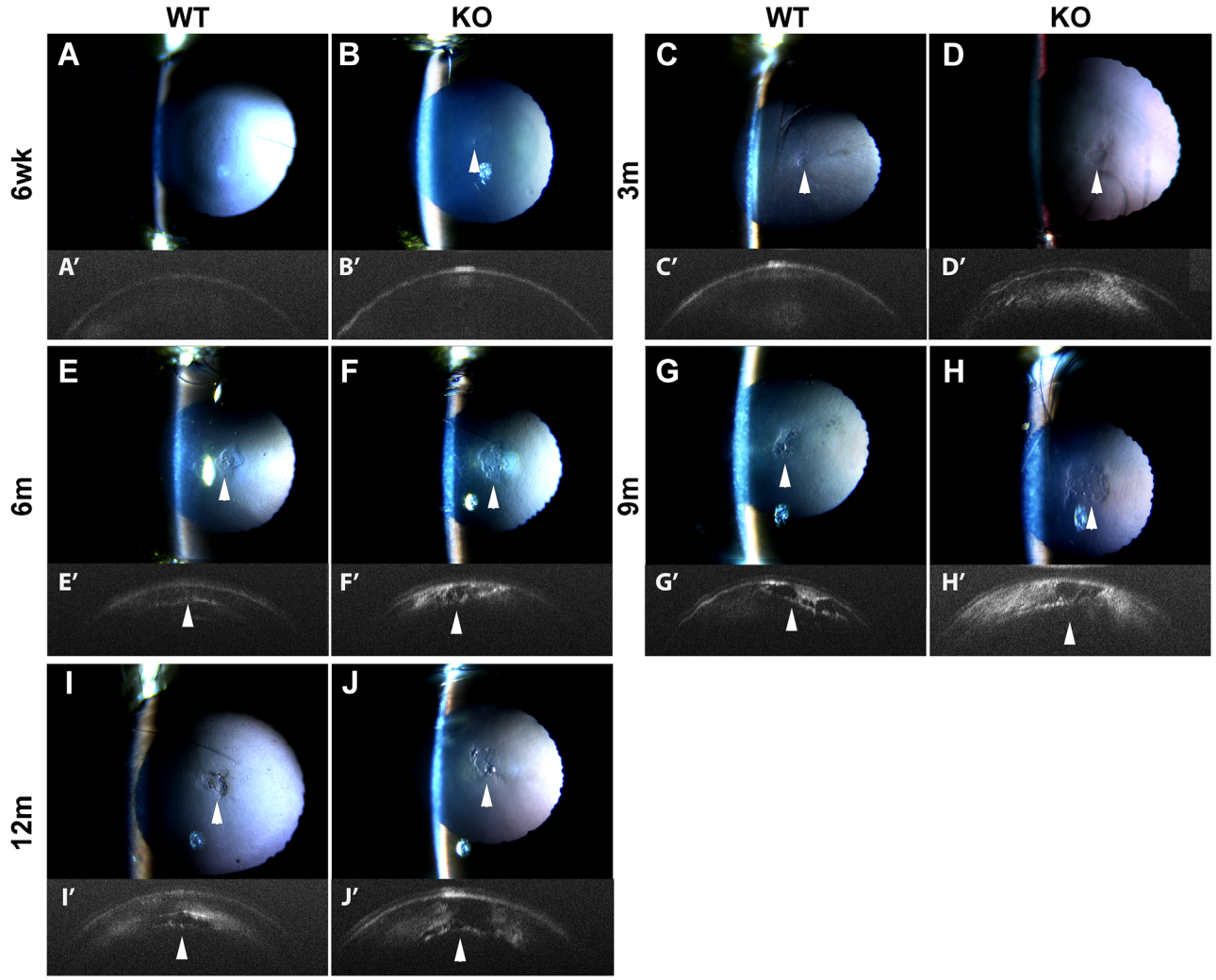

Figure 2. Slit lamp retro-illumination examination of lenses from wild-type and xCT knockout mice. Mice were anaesthetized, pupils dilated, and the lens examined in vivo with a slit lamp where the defects were assessed under retro-illumination and SD-OCT. Images of the lens with cataract observed in wild-type (WT) and knockout (KO) mice at (**A, B**) 6 weeks, (**C, D**) 3 months (**E, F**) 6 months, (**G, H**) 9 months, and (**I, J**) 12 months highlighting the anterior cataract. (**A'–J'**) Representative SD-OCT images of the lesion. *Arrowheads* highlight the presence of vacuoles that were present in the lens cortex; $n = 17$ WT and 18 KO mice at 6 weeks; 10 WT and 10 KO mice at 3 months; 8 WT and 7 KO mice at 6 months; 28 WT and 28 KO mice at 9 months; and 20 WT and 20 KO mice at 12 months.

developed with advancing age in both WT and xCT KO mice lenses. Characterization and localization of these two distinct cataract phenotypes are detailed below.

Punctate Nuclear Cataracts are a Natural Feature in Both WT and xCT KO Mice. Using slit lamp parallelepiped examination, tiny white punctate dots were detected in the nucleus of both WT and xCT KO mice lenses at 6 weeks, 3 months, 6 months, 9 months, and 12 months of age (Figs. 1A–J; arrows) and their appearance did not change with age. The number of animals that presented with these dots were similar from 6 weeks to 12 months of age for WT and xCT KO mice lenses (Fig. 1K; see Supplementary Table S1 for count). Comparing between genotype revealed no significant differences in the frequency (Fig. 1K).

Anterior Cataracts are a Feature of Aging in WT and xCT KO Mice, but are More Prevalent in xCT KO Mice. Using parallelepiped illumination, a second cataract phenotype was localized to the anterior region of the lens, which first became obvious at 3 months of age in the xCT KO lenses (Fig. 1D; arrowhead). While visible using parallelepiped illumination, this cataract type was more prominent and easily visualized using retro-illumination (Figs. 2A–J). At 6 weeks of age, while the majority of WT mice lenses ($n = 17$) and xCT KO mice ($n = 18$) lenses were clear and transparent (see Fig. 2A), a subtle pinpoint defect was detected in 2 WT mice and 2 xCT KO mice lenses (see Fig. 2B; arrowhead). At 3 months of age, a distinct and vacuole-like granular cataract was observed in some WT mice ($n = 4/10$) and the majority of xCT KO mice ($n = 9/10$) lenses (see Figs. 2C–D; arrowhead). At 6 to 12 months of age, cataracts were detected (Figs. 2E–J; arrowhead) in the majority of WT and xCT KO mice lenses (Fig. 3A; see Supplementary Table S1 for count) The vacuole-like appearance of these cataracts was confirmed using spectral-domain (SD)-OCT (Figs. 2D'–J'). In lenses from mice 3 months of age, areas of hypo and hyper reflectivity were seen highlighting the nonhomogeneous structure of the lens affected with this type of cataract (Figs. 2D'–J'; arrowhead). The number

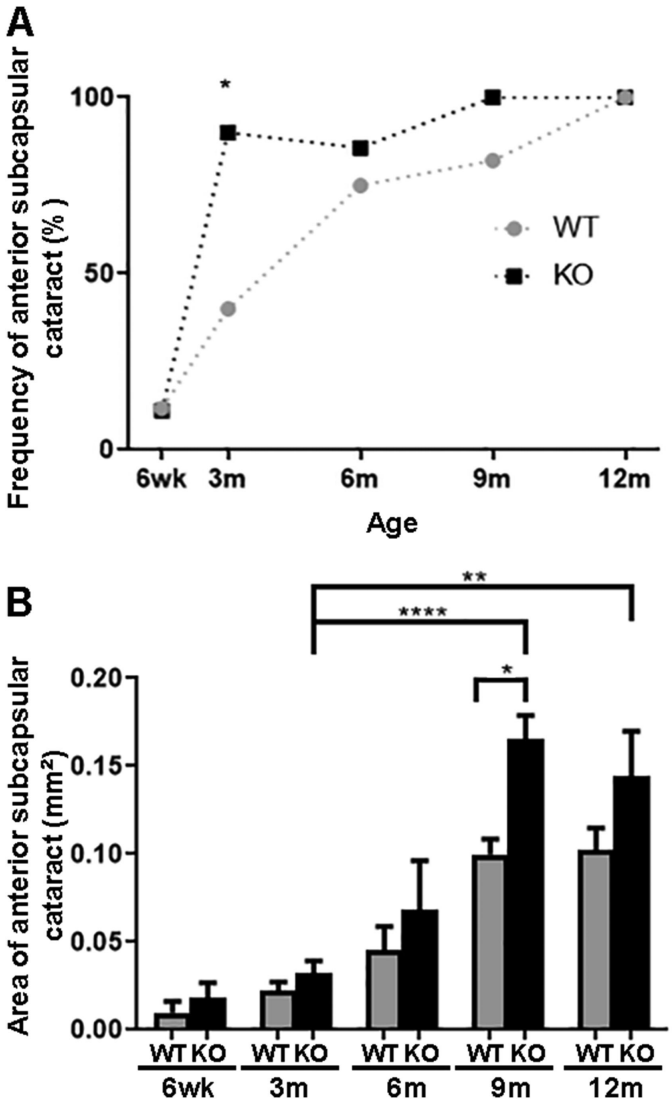

Figure 3. Comparison of anterior cataract frequency and cataract lesion area in wildtype and xCT knock mice Images of lenses captured using slit lamp retro-illumination were further assessed to quantify the frequency and area of the anterior cataract in wildtype (WT, *grey*) and knockout (KO, *black*) mice at 6 weeks, 3 months, 6 months, 9 months, and 12 months of age. (**A**) Frequency of the anterior cataract in WT and KO mice (n = 17 WT and 18 KO mice at 6 weeks, 10 WT and KO mice at 3 months, 8 WT and 7 KO mice at 6 months, 28 WT and KO mice at 9 months, and 20 WT and KO mice eyes at 12 months). (**B**) Average area of cataract in lenses that presented with a lesion, n = 2 WT and 2 KO mice at 6 weeks, 4 WT and 9 KO mice at 3 months, 6 WT and 6 KO mice at 6 months, 23 WT and 28 KO mice at 9 months, and 20 WT and 20 KO mice at 12 months. Data expressed in mean ± SEM. *P < 0.05, **P < 0.01, ****P < 0.0001.

of lenses with this anterior cataract increased with age in both WT and xCT KO mice (Fig. 3A). Moreover, the area of the cataract appeared to increase with age in both WT and xCT KO mice but this was significant only in xCT KO mice lenses from 3 months (0.03 mm^2) to 9 months (0.16 mm^2; P < 0.0001) and 3 months to 12 months (0.14 mm^2; P < 0.01; Fig. 3B).

Comparing between genotypes, at 6 weeks of age, the frequency of this type of cataract was similar between WT and xCT KO mice lenses; approximately 11 to 12% (see Fig. 3A). However, at 3 months, the number of lenses with cataracts in the xCT KO mice (90%) was significantly greater when compared to WT mice (40%; P < 0.05), suggesting that the loss of xCT exacerbates cataract formation. At 6 months of age, the majority of WT mice lenses contained a cataract, with the number of lenses with cataracts similar between WT and xCT KO mice. Although the frequency of the cataract was similar between WT and xCT KO mice at 9 months of age, the area of the cataract was significantly increased in the xCT KO mice compared to the WT mice (0.17 vs. 0.1 mm^2, P < 0.05; see Fig. 3B). By 12 months, all WT and xCT KO mice lenses contained an anterior cataract. Although the average area was larger in the xCT KO mice (0.14 mm^2) than WT mice (0.10 mm^2), this difference was not statistically significant.

Anterior Cataracts are Difficult to Visualize In Vitro

Following in vivo assessment, mice were euthanized, eyes enucleated, and the lens dissected from the globe, imaged,

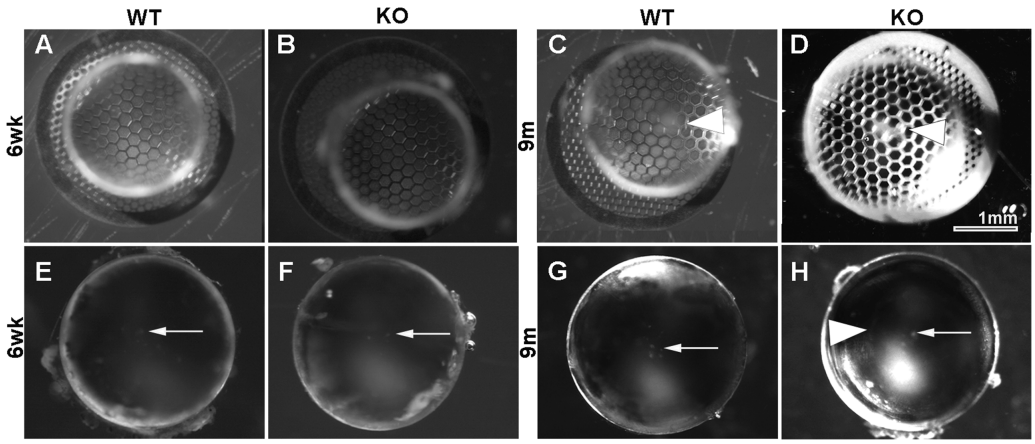

Figure 4. In vitro analysis of lens transparency in wildtype and xCT knockout mice. Mice were euthanized, the eyes were enucleated, the lenses dissected out and imaged under brightfield (top panel) or darkfield microscopy (bottom panel) to visualize optical irregularities and opacities, respectively. Representative images of brightfield microscopy of (**A, B**) 6 week wildtype (WT) and knockout (KO) mice lenses showing clear lenses and (**C, D**) 9 month WT and KO mice lenses on a grid. *Arrowheads* of 9 months highlight distortion of the grid created by the anterior cataract. Representative images of darkfield microscopy on WT and KO (**E, F**) 6 weeks, and (**G, H**) 9 month lenses. Arrows point to the background dot cataract seen in the core of the lens. *Arrowheads* highlight the demarcation created by the anterior cataract; $n = 8$ to 10 lenses/group.

and weighed. For both WT and xCT KO mice lenses, from 6 weeks of age, the weight of the lens steadily increased with age until 6 months, and then remained unchanged until 12 months of age, with no difference in lens wet weight between genotypes for each age group (see Supplementary Table S1).

Lenses were then examined in vitro and imaged using a brightfield microscope with a honeycomb grid placed underneath the lens (Figs. 4A–D). It was difficult to detect distortions by this method and, in some cases, lenses appeared optically normal even when a cataract had previously been identified in vivo. The distortions, however, were more noticeable in the older xCT KO mice lenses, but were relatively subtle and restricted to the central areas (see Figs. 4C–D; arrowhead), consistent with in vivo findings. In an attempt to further visualize lens opacities, lenses were imaged without the grid. Like the distortions, these opacities were very difficult to detect (Figs. 4E–H). Although tiny white dots were detected (see Figs. 4E–H; arrows), there were no obvious opacities except for a faint demarcation that looked like the margins of the anterior cataract in the 9 m xCT KO mice lens (see Fig. 4H; arrowhead).

Lens Morphology is Disrupted at the Anterior Poles of WT and xCT KO Mice Lenses

To investigate lens morphology, WT and xCT KO mice lenses were fixed, cryoprotected, sectioned in the axial orientation, labeled with WGA and DAPI, and then viewed under a confocal microscope. Representative low magnification images of a 6-week-old WT mouse lens with no cataract shows a regular arrangement of lens epithelial and fiber cells (Fig. 5A), whereas the a 9-month-old xCT KO mouse with a cataractous lens showed confined disruption of fiber cell arrangement in the anterior region of the lens (Fig. 5B; asterisk). High magnification images of 6-week and 3-month-old WT mice sections revealed the epithelium and fiber cell structure to appear normal with the ends of the fiber cells meeting at the sutures (Figs. 5C–E). However, in 6-month-old WT mice lenses, damage to the lens fiber cells were detected, which was visible as a large vacuole and appeared to be a result of fiber cell swelling underneath the anterior epithelium (Fig. 5G). In xCT KO mice lenses, whereas lens morphology appeared normal at 6 weeks of age, cell swelling in the anterior region was detected at 3 months of age (Fig. 5F). At 6 months, the damage was more extensive with fiber cell disruption evident deeper into the cortex region (Fig. 5H). A similar finding to the 6-month-old xCT KO mice lens was also apparent in 9-month and 12-month-old WT and xCT KO mice lenses (Figs. 5I–L).

Anterior Cataracts are Atypical of Epithelial Mesenchymal Transition-Anterior Subscapular Cataracts. A typical anterior subcapsular cataract results from aberrant growth and epithelial mesenchymal transition (EMT) to form fibrotic plaques. Cells within these subcapsular plaques express extracellular matrix and cytoskeletal proteins not normally synthesized by lens cells, including α-SMA.[27] To determine whether WT and xCT KO mice lenses exhibited typical EMT anterior subscapular cataract characteristics, 9-month WT and xCT KO mice lenses with were fixed, cryoprotected, and cryosectioned in the axial orientation to visualize the anterior epithelium. WT and xCT KO mice axial lens sections were then labeled with α-SMA and DAPI (Fig. 6).

Labeling of DAPI in WT and xCT KO mice lenses did not reveal the presence of multi-nuclei associated with plaque formation that are typical of anterior cataract.[27,28] Furthermore, WT and xCT KO mice lenses exhibited very faint labeling for α-SMA (see Fig. 6).

xCT KO Mice Show no Signs of Increased Oxidative Stress Biomarkers

We next investigated the mechanisms that may contribute to the accelerated onset of this anterior cataract by examining markers of oxidative stress, such as lipid peroxidation and protein carbonyl formation in whole lenses (Fig. 7).

Investigative Ophthalmology & Visual Science

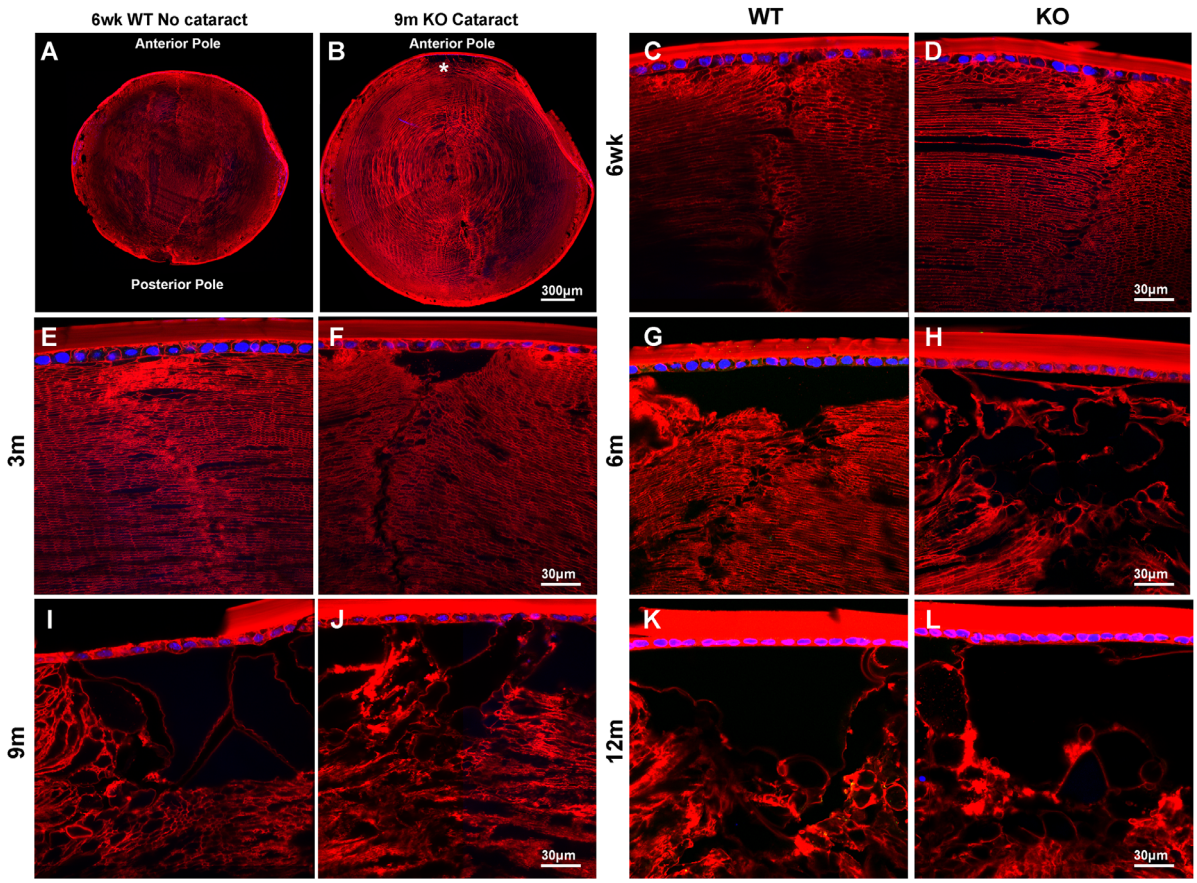

Figure 5. Comparison of morphology of the anterior pole of lenses from wildtype and xCT knockout mice. Lenses were fixed and then cryosectioned in an axial orientation and sections labelled with DAPI, to highlight the nuclei (*blue*), and WGA (*red*), to visualize fiber cell morphology. (**A**) Low magnification image of a 6 week wild-type (WT) mouse lens with no cataract and (**B**) 9 month knockout mouse (KO) lens depicting localized changes at the anterior pole. Representative high magnification images of fiber cell morphology at the anterior pole of the lenses are shown at (**C, D**) 6 weeks, (**E, F**) 3 month, (**G, H**) 6 months, (**I, J**) 9 months, and (**K, L**) 12 months for WT **C, E, G, I, K** and KO **D, F, H, J, L** mice. No multilayered nuclei were present. Asterisks (*) highlights confined disruption of fiber cells, $n = 2$ to 3 lenses/group.

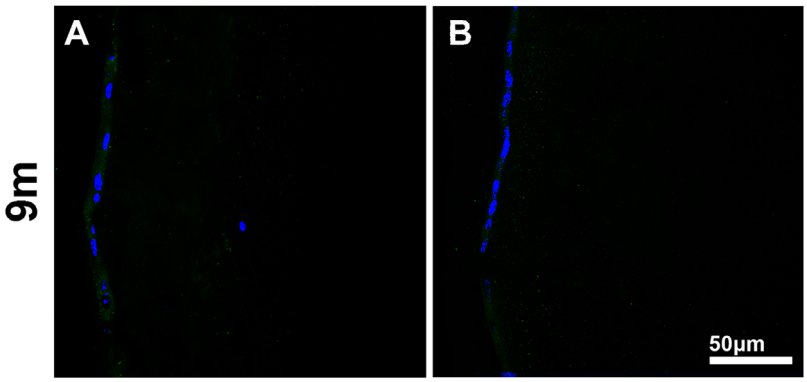

Figure 6. Comparison of α-smooth muscle actin in lenses from wildtype and xCT knockout mice. Lens sections were fixed, cryosectioned, and labelled with DAPI (*blue*) and α-SMA antibodies (*green*). Representative images of the central anterior region for (**A**) WT and (**B**) KO mice in 9 month lenses with cataract show that α-SMA labeling was faint and no multilayered nuclei were present; $n = 2$ lenses/group.

With age, 4-HNE levels were similar from 6 weeks to 12 months in the WT mouse. In the xCT KO mouse, 4-HNE levels were significantly increased from 6 weeks to 9 months ($P < 0.05$), 3 months to 9 months ($P < 0.05$), and 6 months to 9 months ($P < 0.05$) of age (see Fig. 7A). This suggests that 4-HNE appears to increase with age, more so in the xCT KO mice compared to the WT mice. Comparing between genotypes, 4-HNE levels were similar and no significant

Investigative Ophthalmology & Visual Science

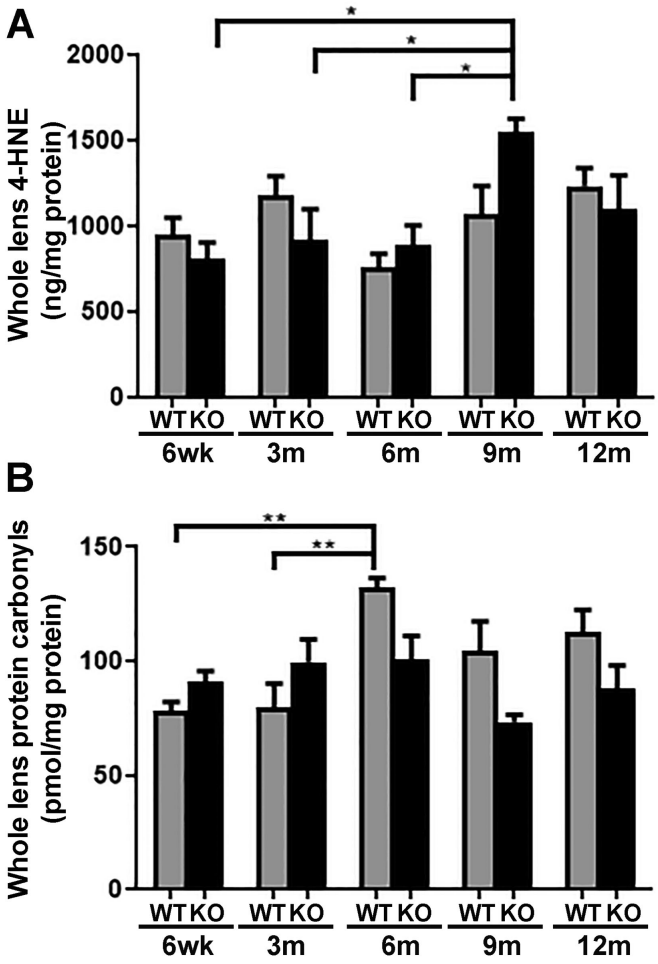

Figure 7. Comparison of oxidative stress markers 4-HNE and protein carbonyl levels in lenses from wildtype and xCT knockout mice. Using ELISA-based assays, oxidative stress markers from whole lens homogenates of 6 weeks, 3 months, 6 months, 9 months, and 12 months wildtype (WT, *grey*) and knockout (KO, *black*) lenses were quantified for (**A**) 4-HNE and (**B**) protein carbonyls. Data expressed in mean ± SEM; *$P < 0.05$, **$P < 0.01$; $n = 5$ to 6/group.

differences were found between WT and the xCT KO mice for all age groups (see Fig. 7A; see Supplementary Table S1 for raw data).

Protein carbonyl (PC) levels increased in the WT mice from 6 weeks to 6 months ($P < 0.01$) and 3 months to 6 months ($P < 0.01$), but no differences were seen with age in the xCT KO mouse (Fig. 7B). Between genotypes, it appeared that the WT mice had higher protein carbonyl levels compared to the xCT KO mouse at 6 months, 9 months, and 12 months of age, but these differences were not statistically significant (see Fig. 7B; see Supplementary Table S1 for raw data). Overall, these results suggest that the loss of xCT does not significantly result in increased oxidative stress in the lens.

xCT KO Mice Lenses Show Decreased Levels of GSH in the Epithelium But Not in the Cortex or Nucleus

Because in vitro studies have shown xCT to be important in providing a source of intracellular cyst(e)ine for GSH synthesis,[14,17] we next investigated whether loss of xCT results in change in intracellular GSH levels in the lens (Fig. 8). First, whole WT and xCT KO mice lenses at the five different age groups were homogenized and assessed for GSH content using LC-MS/MS. With age, GSH levels did not change in the WT or xCT KO mice lenses (see Supplementary Table S1 for raw data). Comparison between genotypes revealed that GSH levels were similar between WT and xCT KO mice lenses for each age group (Fig. 8A), suggesting that GSH levels are maintined in the absence of xCT. GSSG levels were minimal in WT and xCT KO mice lenses for all age groups (ranging from 0–0.40 µmol/g w/w), with no differences in GSSG levels between WT and xCT KO mice lenses at each age group (Fig. 8B).

Because we had shown previously that xCT expression was localized to the lens epithelium and outer cortex,[22] and given in this study that loss of xCT results in the accelerated fomation of an anterior cataract, we wondered if changes in GSH levels may be restricted to the anterior regions of the lens. To investigate this, we dissected the lens into the epithelium, cortex, and nucleus and analyzed GSH levels in these different regions. With age, in the WT mice lens epithelium (Fig. 8C), GSH levels significantly increased at 3 months of age compared to 6 weeks of age ($P < 0.001$; see Supplementary Table S1 for raw data). GSH levels then significantly decreased at 6 months of age compared to 3 months

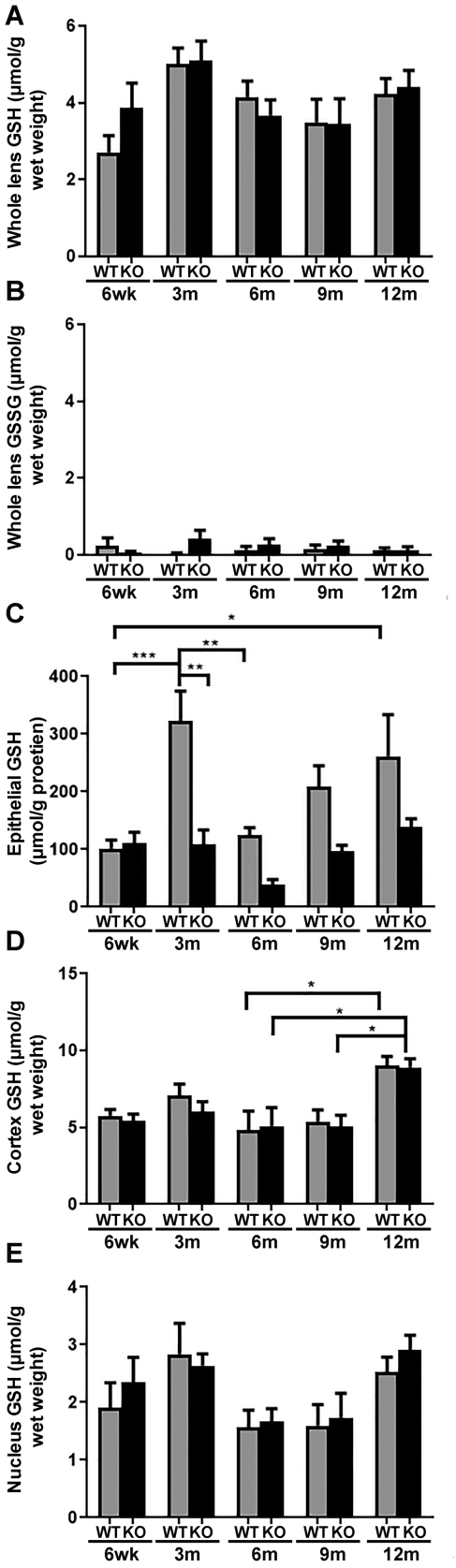

Figure 8. Comparison of intracellular GSH levels in lenses of wildtype and xCT knockout mice. The supernatant from whole lens homogenates or homogenates of the epithelium, cortex, and nucleus were incubated in the presence or absence of TCEP and derivatized using MBrB to quantify total GSH (GSH + GSSG) and reduced GSH using LC-MS/MS in 6 weeks, 3 months, 6 months, 9 months, and 12 months of age wildtype (WT, *grey*) and knockout (KO, *black*) mice. (**A**) GSH concentrations in whole lenses. (**B**) Lens GSSG concentration were quantified. GSH levels in the (**C**) epithelium, (**D**) cortex, (**E**) and nucleus were quantified. Data expressed in mean ± SEM. *$P < 0.05$, **$P < 0.01$, or ***$P < 0.001$. For GSH and GSSG in whole lenses $n = 6$ WT and 6 KO mice at 6 weeks; $n = 8$ WT and KO mice at 3 months; $n = 9$ WT and KO mice at 6 months, $n = 6$ WT and 6 KO mice at 9 months, $n = 5$ WT and 5 KO mice at 12 months. For epithelial, cortex, and nucleus GSH; $n = 6$/group.

of age ($P < 0.01$) and then remained similar at 9 months and 12 months of age compared to that of the 6 month age group (see Fig. 8C). In the xCT KO mice lens epithelium, GSH levels did not change from 6 weeks to 12 months of age (see Fig. 8C). Although there appeared to be a decrease in GSH levels at 6 months of age, this was not statisically signficant. Between genotypes in the epithelium, GSH levels were similar between 6 week WT and xCT KO mice (see Fig. 8C). A two-fold or more decrease in GSH levels was detected in the 3 month, 6 month, 9 month, and 12 month old xCT KO mice. However, this decrease was only significant at 3 months of age ($P < 0.01$).

In the cortex (Fig. 8D), WT GSH levels were similar with age with the exception of the 12-month-old lens, where GSH levels were significantly higher compared to the 6 month old age group ($P < 0.05$). In the xCT KO mice, GSH levels were similar for each age group except at 12 months where GSH levels were significantly higher compared to 6 month ($P < 0.05$) and 9 month ($P < 0.05$) old mice (see Supplementary Table S1 for raw data). There were no differences in GSH levels in the cortex between WT and xCT KO mice lenses for each age group (see Fig. 8D)

In the nucleus (Fig. 8E), GSH levels were similar with age, from 6 weeks to 12 months in both WT and xCT KO mice lenses and no differences in GSH levels were seen between WT and xCT KO mice lenses for all age groups (see Supplementary Table S1 for raw data).

These results suggest that although the loss of xCT does not alter GSH levels in whole lenses, a localized decrease is seen in the epithelium as early as 3 months of age in the xCT KO mice.

xCT KO Mice Exhibit an Oxidative Shift of Cystine/Cysteine Balance in the Aqueous Humour

We have previously shown that the aqueous humour of 6-week-old xCT KO mice contained significantly higher cystine levels compared to age matched WT mice, whereas cysteine levels remained unchanged between WT and xCT KO mice.[22] This was indicative of an oxidative shift in the aqueous cystine/cysteine balance in the xCT KO mouse. To investigate whether this effect is maintained with advancing age, we extended our initial measurements of cystine and cysteine concentrations in the aqueous humour of WT and xCT KO mice to animals of 3 months, 6 months, 9 months, and 12 months of age.

Cysteine levels were similar with age from 6 weeks to 12 months in both WT and xCT KO mice. Comparing between genotypes, cysteine levels did not differ between WT and xCT KO mice for each age group (Fig. 9A).

Cystine levels in the WT mice were also similar with age from 6 week to 12 months (Fig. 9B; grey). Although it appears that there is an increase in cystine levels from

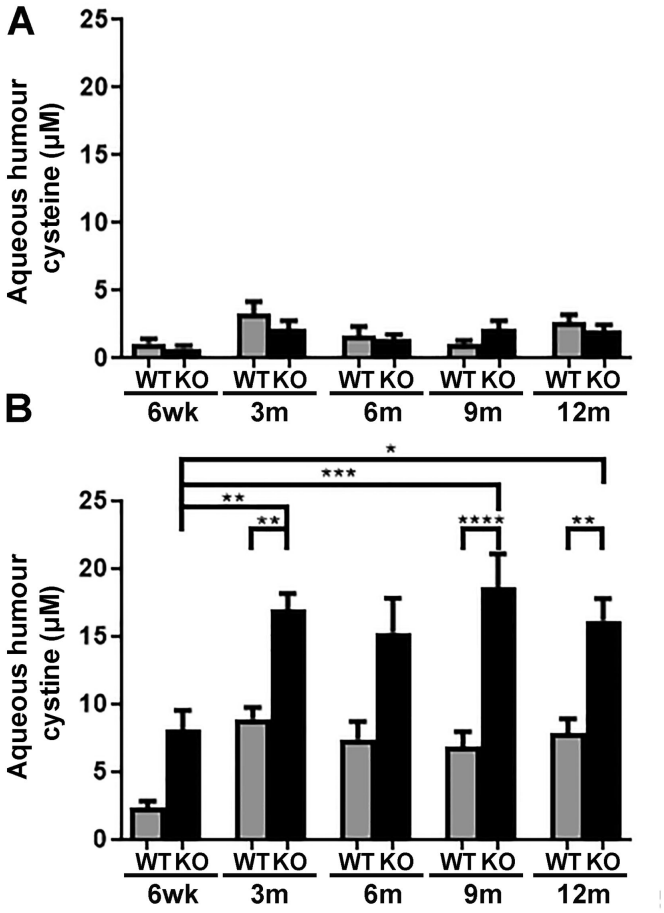

Figure 9. Comparison of cysteine and cystine concentrations in the aqueous humour of wildtype and xCT knockout mice. Aqueous humour was collected from 6 weeks, 3 months, 6 months, 9 months, and 12 months wildtype (WT, *grey*) and xCT knockout (KO, *black*) eyes and incubated in the presence or absence of TCEP and then derivatized with MBrB to quantify total cysteine (cystine + cysteine) and reduced cysteine using LC-MS/MS. (**A**) Aqueous cysteine levels were similar between age and genotype. (**B**) Aqueous cystine levels increased with age in the KO mice and were elevated in the KO mouse when compared to age-matched WT animals. Data expressed in mean ± SEM. $^{*}P < 0.05$, $^{**}P < 0.01$, $^{***}P < 0.001$, or $^{****}P < 0.0001$; $n = 6$ WT and KO mice at 6 weeks, 9 WT and KO mice at 3 months, 6 WT and KO mice at 6 months, 8 WT and KO mice at 9 months, and 12 WT and KO mice at 12 months.

6 weeks to 3 months, this was not statistically significant. However, in the xCT KO mice (see Fig. 9B; black), cystine levels were significantly increased at 3 months ($P < 0.01$), 9 months ($P < 0.0001$), and 12 months ($P < 0.01$) compared to 6-week-old mice. Comparing between genotypes revealed cystine levels to be elevated in the xCT KO mice compared to the WT mice (see Fig. 9B) at 6 weeks (3.5-fold increase), 3 months (1.9-fold increase), 6 months (2.1-fold increase), 9 months (2.7-fold increase), and 12 months of age (2.0-fold increase). However, this was only statistically significant at 3 months ($P < 0.01$), 9 months ($P < 0.0001$), and 12 months of age ($P < 0.001$).

Taken together, these findings show that although loss of xCT does not alter cysteine levels, cystine levels are significantly increased in the aqueous humour.

Discussion

In this study, we investigated the in vivo role of xCT in the lens using a global xCT KO mouse. We achieved this by performing in vivo eye examinations and immunohistochemistry to characterize the effects of loss of xCT on lens transparency and morphology. We also used a combination of mass spectrometry and biochemical assays to quantify cystine/cysteine levels in the aqueous humour and GSH/GSSG levels and oxidative stress biomarkers in the lenses of WT and xCT KO mice at different ages.

First, we assessed the impact of loss of xCT on lens transparency. In vivo examination of the lenses of anesthetized WT and xCT KO mice revealed two types of cataracts present in both WT and xCT KO mice. The first type of cataract was a punctate cataract located in the nucleus of the lens. The size and number of lenses with this type of cataract did not differ with age or genotype, suggesting that this is a natural feature in the C57BL/6 background mice, and that loss of xCT does not affect the development of this cataract. This type of cataract was noted in a study that examined 4-month-old C57Bl/6 mice,[29] but no further details about this cataract was given. Although this punctate nuclear cataract is obvious on slit lamp examination, this cataract was not detectable by brightfield imaging. It was visible as subtle pinpoint lesions on darkfield imaging (see Fig. 4) and easily missed if not focused at the nucleus of the lens.

The second type of cataract detected was an anterior cataract, which was phenotypically distinct from an anterior

Investigative Ophthalmology & Visual Science

subcapsular cataract defined by aberrant epithelial cell proliferation and the presence of subcapsular plaques.[27] This type of cataract was detected in both WT and xCT KO mice and although it appeared to be a natural feature of aging in mice of the C57BL/6J background, loss of xCT appeared to exacerbate the frequency and size of the cataract (see Fig. 3). It was initially detected as a tiny pinpoint lesion at the anterior pole, in 3-month-old xCT KO mice and evident in the 6-month-old WT and xCT KO mice. A search of the literature revealed two other studies that reported a natural formation of a similar anterior cataract in C57BL/6J mice. However, both studies examined the lenses in vitro using darkfield microscopy and examined mice at 12 months of age and over.[30,31] By using in vivo retro-illumination on the slit-lamp on mice ranging from 6 weeks to 12 months of age, we noted the onset of the cataract much earlier than that reported by Zhang et al.[30] and Cheng et al.,[31] hence, it is possible that these changes to the anterior pole region may have been missed in younger mice by examining the lens in vitro. It was found in our study that the in vivo irregularities observed by slit lamp were not easily detectable in vitro using brightfield imaging.

Morphological studies revealed that these anterior cataracts in both WT and xCT KO mice presented as large vacuoles in the central anterior area of the lens. However, with immunohistochemistry, the damage appeared to be associated with localized fiber cell swelling and disruption at the anterior pole and not associated with epithelial mesenchymal transition seen in typical anterior subcapsular cataract. Cheng et al. reported similar morphological findings in older 18-month-old C57BL/6 mice where a lack of epithelial mesenchymal transition was also noted along with fiber cell disruption and a lack of fusion of the fibers at the anterior Y sutures.[31]

In our study, the frequency of these anterior cataracts in the xCT KO mice was significantly greater compared to the WT mice with vacuoles first manifesting at 3 months of age. The percentage of lenses affected in 3 month xCT KO mice was equivalent to the percentage of lenses affected in 12 month WT mice. This suggests that although the anterior cataract appears to be age related, the development of this cataract is accelerated in the KO mice, suggesting that the KO mice lens are aging faster than the WT mice lens. Additionally, the disruption to fiber lens morphology was more extensive in the xCT KO mice relative to age-matched WT mice lenses with the size of the cataract much larger in the 9 and 12 month xCT KO mice than WT mice. We suspected that this might lead to weight differences between the two genotypes, however, due to the confined and localized nature of the anterior cataract, no differences in lens weight were found between WT and xCT KO mice lenses for all age groups.

In investigating the molecular mechanisms associated with anterior cataract, GSH levels in the whole lenses were surprisingly similar between the two genotypes. Likewise, 4-HNE levels in the whole lens were also similar between WT and xCT KO mice. Although GSH levels in the whole lenses were maintained in the absence of xCT (see Fig. 8A), GSH levels in the lens epithelium were significantly decreased in 3 month xCT KO mice lenses compared to the WT mice (see Fig. 8C). This decrease was also evident at 6 months, 9 months, and 12 months, although it was not statistically significant (see Fig. 8C). The difference in GSH levels observed in the epithelium of the xCT KO mice was not seen in the cortex or nucleus of the xCT KO mice lens, which may explain why antioxidant levels and oxidative stress markers (4-HNE and protein carbonyls; see Fig. 7) in whole lenses did not appear to be different between the genotypes. Additionally, the localized decrease of GSH in the epithelium correlates with the restricted expression of xCT in this region (see Supplementary Fig. S2) suggesting that xCT is important in maintaining GSH levels in the epithelium. Of note, we cannot rule out localized changes in the oxidative markers (4-HNE and protein carbonyl) in the xCT KO mice epithelium and further experiments need to be conducted to confirm this. Furthermore, the accelerated frequency of the anterior cataract at 3 months of age in the xCT KO mice lens (see Fig. 3A), coincides with the first signs of morphological damage (see Fig. 5F) and loss of GSH in the lens epithelium (see Fig. 8C).

Although xCT is also expressed in the cortical fiber cells, we did not see a decrease in GSH levels in the cortex. In other studies, GSH content in the cerebrum, cerebellum, hippocampus, striatum, liver, kidneys, thymus, spleen, lungs, heart, and pancreas of the xCT KO mice were similar to that of the WT mice, indicating that in the absence of xCT, these tissues were able to accumulate cyst(e)ine and/or maintain GSH levels via alternative mechanisms.[4,5,24,32] A number of alternative pathways exist in the lens that may be utilized to maintain GSH levels in the absence of xCT. For example, it is known that the lens contains the molecular machinery to take up cysteine directly via cysteine uptake transporters,[14,17–19,33] synthesize cysteine via the transsulfuration pathway,[34] or directly uptake GSH via putative GSH transporters.[35] Together, these alternative mechanisms may be upregulated to compensate for the loss of GSH in the cortex, and may explain why no differences were seen in GSH levels in the cortex and the lens as a whole.

Finally, measurement of cystine/cysteine levels in the aqueous humour of WT and xCT KO mice revealed that cystine levels are elevated in xCT KO mice compared to WT mice at all age groups (see Fig. 9B). As cysteine levels remain the same between the WT and xCT KO mice, the elevated levels of cystine results in an imbalance in the cystine/cysteine redox state leading to a more oxidized environment. In addition to lowered GSH levels in the lens epithelium at 3 months, this oxidized environment may also contribute to the earlier onset of the anterior cataract in the xCT KO mouse.

Furthermore, it is interesting to speculate as to which tissues are also responsible for maintaining redox balance in the aqueous humour. Although it is likely that the changes in the humour are a reflection of the plasma, the lens may also play a role in the regulating cystine/cysteine redox balance. In addition to the lens, the ciliary body will also contribute to cystine/cysteine redox balance in the aqueous humour because it is responsible for production of the aqueous humour. Although we were not able to confirm labeling of xCT in the mouse ciliary body,[22] it has been shown in the rat ciliary body that xCT is present in the nonpigmented epithelium; the layer that is in direct contact with the aqueous humour.[20] It is also possible that given the location of xCT in the mouse lens epithelium and cortex (see Supplementary Fig. S2), the lens may work with the ciliary body to maintain cystine/cysteine redox balance in the aqueous humour. Because we are using a global KO mouse, further studies involving the use of a lens conditional KO mouse model would help to confirm the contribution of xCT in the lens in maintaining cysteine/cystine redox balance in the aqueous humour.

Investigative Ophthalmology & Visual Science

In conclusion, in this study, we discovered that genetic deletion of xCT causes an oxidative shift of the aqueous humour and localized depletion of GSH, which may contribute to the early onset of an anterior cataract. The accelerated development of an anterior cataract in xCT KO mice, demonstrates the xCT mouse to be a useful animal model to study the pathophysiology of age-related cataract and to test therapeutic interventions that restore extracellular and intracellular redox balance. Additionally, the xCT KO mouse may also be a useful model to identify the impact of loss of xCT on the other tissues of the eye.

Acknowledgments

The authors thank Hideyo Sato for providing us with the xCT KO mice. They would also like to thank Martin Middleditch for the development of the LC-MS/MS protocol.

Funding from Auckland Medical Research Fund, the Faculty Research Development Fund from the University of Auckland, the Maurice and Phyllis Paykel Trust, the New Zealand Optometric Vision Research Foundation, the Hope Foundation for Research on Ageing, and the New Zealand Association of Optometrists.

Disclosure: **R.M. Martis**, None; **B. Li**, None; **P.J. Donaldson**, None; **J.C.-H. Lim**, None

References

1. Bannai S, Kitamura E. Transport interaction of L-cystine and L-glutamate in human diploid fibroblasts in culture. *J Biol Chem.* 1980;255:2372–2376.
2. Baker DA, McFarland K, Lake RW, et al. Neuroadaptations in cystine-glutamate exchange underlie cocaine relapse. *Nat Neurosci.* 2003;6:743.
3. Baker DA, Xi Z-X, Shen H, Swanson CJ, Kalivas PW. The origin and neuronal function of in vivo nonsynaptic glutamate. *J Neurosci.* 2002;22:9134–9141.
4. De Bundel D, Schallier A, Loyens E, et al. Loss of system xc- does not induce oxidative stress but decreases extracellular glutamate in hippocampus and influences spatial working memory and limbic seizure susceptibility. *J Neurosci.* 2011;31:5792–5803.
5. Massie A, Schallier A, Kim SW, et al. Dopaminergic neurons of system xc- deficient mice are highly protected against 6-hydroxydopamine-induced toxicity. *J FASEB.* 2011;25:1359–1369.
6. La Bella V, Valentino F, Piccoli T, Piccoli F. Expression and developmental regulation of the cystine/glutamate exchanger (xc-) in the rat. *Neurochem Res.* 2007;32:1081–1090.
7. Pow DV. Visualising the activity of the cystine-glutamate antiporter in glial cells using antibodies to aminoadipic acid, a selectively transported substrate. *GLIA.* 2001;34:27–38.
8. Shih AY, Murphy TH. xCt cystine transporter expression in HEK293 cells: pharmacology and localization. *Biochem Biophys Res Commun.* 2001;282:1132–1137.
9. Van Liefferinge J, Bentea E, Demuyser T, et al. Comparative analysis of antibodies to xCT (Slc7a11): Forewarned is forearmed. *J Comp Neurol.* 2016;2016:1015–1032.
10. Watanabe H, Bannai S. Induction of cystine transport activity in mouse peritoneal macrophages. *J Exp Med.* 1987;165:628–640.
11. Sato H, Tamba M, Ishii T, Bannai S. Cloning and expression of a plasma membrane cystine/glutamate exchange transporter composed of two distinct proteins. *J Bioll Chem.* 1999;274:11455–11458.
12. Dun Y, Mysona B, Van Ells T, et al. Expression of the cystine-glutamate exchanger (xc-) in retinal ganglion cells and regulation by nitric oxide and oxidative stress. *Cell Tissue Res.* 2006;324:189–202.
13. Bridges CC, Kekuda R, Wang H, et al. Structure, function, and regulation of human cystine/glutamate transporter in retinal pigment epithelial cells. *Investig Ophthal Vis Sci.* 2001;42:47–54.
14. Lall MM, Ferrell J, Nagar S, Fleisher LN, McGahan MC. Iron regulates L-cystine uptake and glutathione levels in lens epithelial and retinal pigment epithelial cells by its effect on cytosolic aconitase. *Investig Ophthal Vis Sci.* 2008;49:310–319.
15. Hu RG, Lim J, Donaldson PJ, Kalloniatis M. Characterization of the cystine/glutamate transporter in the outer plexiform layer of the vertebrate retina. *Eur J Neurosci.* 2008;28:1491–1502.
16. Langford MP, Redens TB, Texada DE. Excitatory amino acid transporters, xc- antiporter, γ-glutamyl transpeptidase, glutamine synthetase, and glutathione in human corneal epithelial cells. In: Babizhayev M., Li DC, Kasus-Jacobi A, Žorić L, Alió J, eds. *Studies on the Cornea and Lens.* New York, NY: Springer; 2015:67–82.
17. Langford MP, Redens TB, Liang C, Kavanaugh AS, Texada DE. EAAT and Xc-exchanger inhibition depletes glutathione in the transformed human lens epithelial cell line SRA 01/04. *Curr Eye Res.* 2015;41:1–10.
18. Lim JC, Lam L, Li B, Donaldson PJ. Molecular identification and cellular localization of a potential transport system involved in cystine/cysteine uptake in human lenses. *Exp Eye Res.* 2013;116:219–226.
19. Lim J, Lam YC, Kistler J, Donaldson PJ. Molecular characterization of the cystine/glutamate exchanger and the excitatory amino acid transporters in the rat lens. *Investig Ophthal Vis Sci.* 2005;46:2869–2877.
20. Li B, Umapathy A, Tran LU, Donaldson PJ, Lim JC. Molecular identification and cellular localisation of GSH synthesis, uptake, efflux and degradation pathways in the rat ciliary body. *Histochem Cell Biol.* 2013;139:559–571.
21. Li B, Lee MS, Lee RS, Donaldson PJ, Lim JC. Characterization of glutathione uptake, synthesis, and efflux pathways in the epithelium and endothelium of the rat cornea. *Cornea.* 2012;31:1304–1312.
22. Martis RM, Donaldson PJ, Li B, Middleditch M, Kallingappa PK, Lim JC. Mapping of the cystine–glutamate exchanger in the mouse eye: a role for xCT in controlling extracellular redox balance. *Histochem Cell Biol.* 2019;152(4):293–310.
23. Langford MP, Redmond P, Chanis R, Misra RP, Redens TB. Glutamate, excitatory amino acid transporters, xc- antiporter, glutamine synthetase, and γ-glutamyltranspeptidase in human corneal epithelium. *Curr Eye Res.* 2010;35:202–211.
24. Sato H, Shiiya A, Kimata M, et al. Redox imbalance in cystine/glutamate transporter-deficient mice. *J Biol Chem.* 2005;280:37423–37429.
25. Jacobs MD, Donaldson PJ, Cannell MB, Soeller C. Resolving morphology and antibody labeling over large distances in tissue sections. *Microsc Res Tech.* 2003;62:83–91.
26. Nowak RB, Fischer RS, Zoltoski RK, Kuszak JR, Fowler VM. Tropomodulin1 is required for membrane skeleton organization and hexagonal geometry of fiber cells in the mouse lens. *J Cell Biol.* 2009;186:915–928.
27. Lovicu FJ, Schulz MW, Hales AM, et al. TGFβ induces morphological and molecular changes similar to human anterior subcapsular cataract. *Br J Ophthalmol.* 2002;86:220–226.
28. Wojciechowski MC, Mahmutovic L, Shu DY, Lovicu FJ. ERK1/2 signaling is required for the initiation but not

progression of TGFβ-induced lens epithelial to mesenchymal transition (EMT). *Exp Eye Res*. 2017;159:98–113.

29. Moore BA, Roux MJ, Sebbag L, et al. A population study of common ocular abnormalities in C57BL/6N rd8 mice. *Investig Ophthal Vis Sci*. 2018;59:2252–2261.
30. Zhang J, Yan H, Löfgren S, Tian X, Lou MF. Ultraviolet radiation–induced cataract in mice: The effect of age and the potential biochemical mechanism. *Investig Ophthal Vis Sci*. 2012;53:7276–7285.
31. Cheng C, Parreno J, Nowak RB, et al. Age-related changes in eye lens biomechanics, morphology, refractive index and transparency. *Aging (Albany NY)*. 2019;11:12497.
32. Kobayashi S, Sato M, Kasakoshi T, et al. Cystathionine is a novel substrate of cystine/glutamate transporter implications for immune function. *J Biol Chem*. 2015;290:8778–8788.
33. Lim J, Lorentzen KA, Kistler J, Donaldson PJ. Molecular identification and characterisation of the glycine transporter (GLYT1) and the glutamine/glutamate transporter (ASCT2) in the rat lens. *Exp Eye Res*. 2006;83:447–455.
34. Persa C, Pierce A, Ma Z, Kabil O, Lou MF. The presence of a transsulfuration pathway in the lens: a new oxidative stress defense system. *Exp Eye Res*. 2004;79:875–886.
35. Li B, Li L, Donaldson PJ, Lim JC. Dynamic regulation of GSH synthesis and uptake pathways in the rat lens epithelium. *Exp Eye Res*. 2010;90:300–307.

Investigative Ophthalmology & Visual Science